PERGAMON

International Journal of Solids and Structures 37 (2000) 5579–5597

INTERNATIONAL JOURNAL OF SOLIDS and STRUCTURES

www.elsevier.com/locate/ijsolstr

Thermoelastic behavior of composites with functionally graded interphase: a multi-inclusion model

Jiang Yu Li [1]

Center of Excellence for Advanced Materials, University of California, San Diego, USA

Received 8 August 1999

Abstract

The thermoelastic behavior of composites with functionally graded interphase is analyzed by the multi-inclusion model, where the explicit expressions for the effective thermoelastic moduli and thermoelastic field of the composite are obtained. This method is especially suitable for the analysis of functionally graded interphase because it allows the arbitrary varying material properties in the interphase, allows a wide range of microgeometries of the composite, allows determination of the complete set of thermoelastic moduli and field, and is easy to implement. Its internal-consistency is also examined. Numerical results for the effective thermoelastic moduli and thermoelastic field of SiC reinforced intermetallic matrix are given and discussed to demonstrate the applicability of the method.

Keywords: Thermoelastic behavior; Matrix; Multi-inclusion model

1. Introduction

Functionally graded materials (FGMs) are a new generation of composite materials characterized by a continuously varying property due to a continuous change in the microstructure details from one surface of the material to the other, such as composition, morphology, and crystal structure. The concept of FGM is to take advantage of certain desirable features of each constituent phases and optimize the distribution of material properties such as strength, hardness, thermal resistance, etc., so that the desired responses to given mechanical and thermal loadings are achieved. FGMs can be used to improve fracture toughness of machine tools, wear resistance and oxidation resistance of high temperature aerospace and automotive components, and ballistic efficiency of lightweight armor materials.

There are two major problems in the design of a FGM, aside from that of material selection; one is determining the optimum spatial dependence for material properties, and the other is predicting the

E-mail address: jjli@starlite.ucsd.edu (J.Y. Li).

[1] Present address: California Institute of Technology, Mail Code 104-44, Pasadena, CA 91125, USA.

0020-7683/00/$ - see front matter
PII: S0020-7683(99)00227-9

characteristic of a FGM for a given property profile (Markworth et al., 1995). In this work, we will focus on the thermoelastic behavior of FGMs given a certain property profile, although the method can also be used to study the effect of different property profile on the material behavior. Various techniques have been adopted to analyze the thermal stress in FGMs in the literature, including numerical determination of residual stresses in FGMs based on continuum model (Delfosse et al., 1997), analysis of residual stress in multi-layered FGMs using laminate theory (Shaw, 1998), study of random and discrete microstructures in FGMs by a physically based computational micromechanics model (Dao et al., 1997), analysis of thermal stresses in functionally graded particle-reinforced composite by Mori–Tanaka model (Noda and Nakai, 1998), and a newly proposed higher order micromechanical theory for FGMs with nonuniform fiber spacing that explicitly couples the local and global effects (Aboudi and Pindera, 1996). In general, these techniques are targeting at a particular microgeometry, such as laminated, particle reinforced, or fiber reinforced composites.

In this work we will study the thermoelastic behavior of composites with functionally graded interphase. By the interphase we refer to the phase between matrix and reinforcement with continuously varying material properties. Specially designed interphase are created in modern composites to improve fracture toughness, chemical compatibility, and matching of thermal expansion coefficients between composite constituents. A significant amount of work have been directed to generalize the micromechanics theory of two-phase composite to composite with inhomogeneous interphase between matrix and reinforcement. Hashin (1990) and Qiu and Weng (1991) suggested a recursive method for axial and transverse bulk moduli, generalizing the composite cylindrical assemblage model (Hashin and Rosen, 1964). Benveniste et al. (1989) and Dunn and Ledbetter (1995) applied Mori and Tanaka (1973) method to composite with coated inclusion. Chu and Rokhlin (1995) have extended the generalized self-consistent model (Christensen and Lo, 1979) to composite with multi-layered fibers, where the transverse shear modulus can be obtained by a transfer matrix algorithm. This technique was later adopted by Huang and Rokhlin (1996) to an interphase with continuously varying properties. A closed form solution is obtained by Lutz and Ferrari (1995) for the stresses and displacements in and around fiber of a fibrous composite, taking into account of effect of inhomogeneous interphase. Our work is based on the multi-inclusion model proposed by Nemat-Nasser and Hori (1993) to predict the effective elastic moduli of multi-phase composites, see also Hori and Nemat-Nasser (1994). This model is especially suitable for composite materials with functionally graded interphase, where the interphase can be assumed to be composed of infinite number of layers with similar and coaxial ellipsoidal shape and uniform material properties, so that the strain and stress in the interphase can be estimated by Eshelby's equivalent-inclusion concept (Eshelby, 1957) and Tanaka–Mori theorem (Tanaka and Mori, 1972). The ellipsoidal shape of the interphase enables us to simulate a wide range of microgeometries of composite, ranging from flakes to continuous fibers. Here we have generalized this model to analyze thermoelastic behavior of composite materials so that the effective thermal expansion coefficient and residual stress can be obtained, as well as the effective elastic moduli. The advantages of this method are as follows: (1) the complete set of thermoelastic moduli and thermoelastic field in the composite can be obtained; (2) a wide range of microgeometries can be studied; (3) the formalism is explicit and closed form expression can be obtained if desired; (4) the material properties can be varied in an arbitrary manner, and the temperature distribution is not necessarily uniform.

The paper is organized in the following manner. Basic equations and notation will be introduced in Section 2. The multi-inclusion model will be reviewed and generalized to study the thermoelastic behavior of composite materials in Section 3; some theoretical considerations will also be presented, where the multi-inclusion model is shown to be self-consistent. Composites with functionally graded interphase is then analyzed in Section 4, where the explicit expressions for the effective thermoelastic moduli as well as loading and residual fields of the composite are obtained. Some numerical results and discussions are given in Section 5.

2. Basic equations and notation

Let us consider the static thermoelastic behavior of a multi-phase composite consisting of a matrix, and $n-1$ reinforcements. The constitutive equation for phase r can be expressed as

$$\sigma_r = \mathbf{C}_r\varepsilon_r + \lambda_r\theta, \tag{1}$$

or in inverse form

$$\varepsilon_r = \mathbf{D}_r\sigma_r + \alpha_r\theta, \tag{2}$$

where σ, ε, and θ are the stress and strain tensors, and temperature change with respect to a reference temperature, respectively. $\mathbf{C}$ and $\mathbf{D}$ are elastic stiffness and compliance tensors and are each other's inverse. λ and α are the thermal stress and strain tensors and satisfy relationship $\lambda_r = -\mathbf{C}_r\alpha_r$. The subscript r is used to denote the quantities belonging to phase r; it does not need to be uniform, in general. It is noted that for the time being the temperature change, unlike other field variables, is regarded uniform over the composite.

The effective thermoelastic moduli can be defined for the composite under the assumption of statistical homogeneity, in terms of average stress and strain in the composite

$$\langle\sigma\rangle = \mathbf{C}^*\langle\varepsilon\rangle + \lambda^*\theta \tag{3}$$

and

$$\langle\varepsilon\rangle = \mathbf{D}^*\langle\sigma\rangle + \alpha^*\theta, \tag{4}$$

where the superscript * is used to denote the effective properties of the composite, and $\langle\bullet\rangle = \int_V(\bullet)\,\mathrm{d}V$ denotes an average over a representative volume element.

From now on let us focus on the boundary conditions of applied linear displacement $\mathbf{u} = \varepsilon^0\mathbf{x}$ and uniform temperature change θ. The applied traction boundary condition can be analyzed in a similar manner. For the thermoelastic behavior of heterogeneous materials, it is convenient to split the elastic field into two parts according to the linearity, one due to the applied linear displacement $\mathbf{u} = \varepsilon^0\mathbf{x}$, the loading field I, and the other due to the temperature change θ, the residual field II (Kreher, 1988; Li and Dunn, 1999). In light of this definition and the average strain theorem (see, e.g., Nemat-Nasser and Hori, 1993), the constitutive equations for fields I and II can be written as

$$\langle\sigma^{\mathrm{I}}\rangle = \mathbf{C}^*\varepsilon^0 \tag{5}$$

and

$$\langle\sigma^{\mathrm{II}}\rangle = \lambda^*\theta. \tag{6}$$

Eqs. (5) and (6) show that the effective elastic stiffness tensor and thermal stress tensor can be obtained from the average loading field and residual field, respectively. From Eqs. (5) and (1), and taking into account of zero temperature change, the effective elastic stiffness tensor can be written as

$$\mathbf{C}^* = \sum_{r=1}^{n} f_r\mathbf{C}_r\mathbf{A}_r, \tag{7}$$

where f_r is the volume fraction of phase r, and the elastic strain concentration factor $\mathbf{A}_r$ is defined by

$$\langle\varepsilon_r^{\mathrm{I}}\rangle = \mathbf{A}_r\varepsilon^0. \tag{8}$$

The effective thermal stress tensor can be obtained directly from Eq. (6), if the average stress in the composite caused by the temperature change θ is known. It can also be obtained from the thermal strain concentration factor, noting that the strain in the individual phase does not disappear,

$$\lambda^* = \sum_{r=1}^{n} f_r(\mathbf{C}_r\mathbf{a}_r + \lambda_r), \tag{9}$$

with the thermal strain concentration factor $\mathbf{a}_r$ defined by

$$\langle \varepsilon_r^{\mathrm{II}} \rangle = \mathbf{a}_r\theta. \tag{10}$$

Eqs. (9) and (6) are equivalent. Another way to evaluate the effective thermal stress tensor is through the elastic strain concentration factor $\mathbf{A}_r$. As shown by Levin (1967) and Rosen and Hashin (1970), there is an exact connection between the effective thermal stress tensor and the elastic strain concentration factor

$$\lambda^* = \sum_{r=1}^{n} f_r\mathbf{A}_r^{\mathrm{T}}\lambda_r, \tag{11}$$

where a superscript T is used to denote tensor transpose. A micromechanics model should give identical thermal stress tensor using Eqs. (9) and (11), see Benveniste et al. (1991) and Li (1999).

3. Multi-inclusion model

In this section we will briefly review the multi-inclusion model proposed by Nemat-Nasser and Hori (1993) for the effective elastic moduli of composite materials. We will also generalize this model to analyze the thermoelastic behavior of composite materials. The foundation of multi-inclusion model is the Tanaka and Mori (1972) theorem, that the average field in an annulus embedded in an infinite medium only depends on the shapes and orientations of the ellipsoids. For a similar and coaxial multi-inclusion embedded in an infinite medium with the elastic stiffness tensor $\mathbf{C}$, as shown in Fig. 1, the average strain in region r can be expressed as

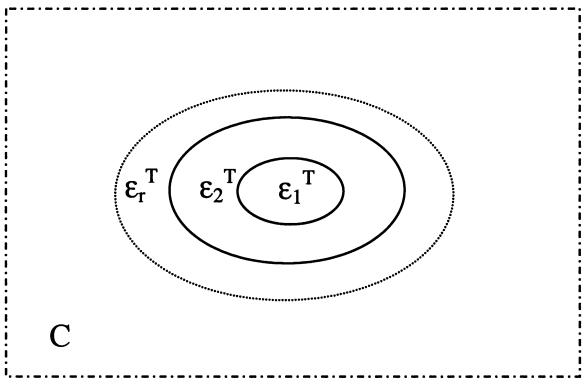

Fig. 1. A multi-inclusion embedded in an infinite medium of elastic moduli $\mathbf{C}$. The eigenstrain in region r is $\varepsilon_r^{\mathrm{T}}$.

$$\langle \varepsilon_r \rangle = \mathbf{S}\langle \varepsilon_r^{\mathrm{T}} \rangle, \tag{12}$$

and the average stress is

$$\langle \sigma_r \rangle = \mathbf{C}(\mathbf{S} - \mathbf{I})\langle \varepsilon_r^{\mathrm{T}} \rangle, \tag{13}$$

where $\varepsilon_r^{\mathrm{T}}$ is the eigenstrain in region r. $\mathbf{S}$ is the Eshelby tensor for the ellipsoidal inclusion, which is a function of the elastic moduli of the infinite medium, $\mathbf{C}$, and the inclusion shape. $\mathbf{I}$ is the fourth-order unit tensor. Note that since the series of ellipsoids are similar and coaxial, they all have identical Eshelby tensor. The basic concept of multi-inclusion model is using the effective moduli of the multi-inclusion to approximate the effective moduli of composite material, represented by the multi-inhomogeneity embedded in an infinite medium, as shown in Fig. 2. The question then is finding the consistent eigenstrain in the multi-inclusion, to make the average field in the multi-inclusion and multi-inhomogeneity equivalent.

3.1. The effective elastic moduli

For the effective elastic moduli, we only need to consider loading field I, the field caused solely by the applied linear displacement. The consistent equation for the multi-inclusion and multi-inhomogeneity is then

$$\mathbf{C}_r\left(\varepsilon^{\infty} + \varepsilon_r^{\mathrm{d}}\right) = \mathbf{C}\left(\varepsilon^{\infty} + \varepsilon_r^{\mathrm{d}} - \bar{\varepsilon}_r^{\mathrm{T}}\right), \tag{14}$$

where ε^{∞} is the uniform strain applied at the boundary of infinite medium, while $\varepsilon_r^{\mathrm{d}}$ is the disturbance strain field due to the presence of the inhomogeneity, and $\bar{\varepsilon}_r^{\mathrm{T}}$ is the equivalent eigenstrain introduced to make the field in the multi-inclusion and multi-inhomogeneity consistent. Eq. (14) can be solved with the disturbance strain field given by Eq. (12) to yield

$$\bar{\varepsilon}_r^{\mathrm{T}} = \Lambda_r \varepsilon^{\infty}, \tag{15}$$

where

$$\Lambda_r = \left[(\mathbf{C} - \mathbf{C}_r)^{-1}\mathbf{C} - \mathbf{S}\right]^{-1}. \tag{16}$$

With equivalent eigenstrain known, the average stress and strain in the multi-inclusion (and thus, multi-inhomogeneity) can be determined from Eqs. (12) and (13), plus the uniform stress and strain in the infinite medium,

$$\langle \varepsilon_r^{\mathrm{I}} \rangle = (\mathbf{I} + \mathbf{S}\Lambda_r)\varepsilon^{\infty} \tag{17}$$

and

$$\langle \sigma_r^{\mathrm{I}} \rangle = \mathbf{C}\left[\mathbf{I} + (\mathbf{S} - \mathbf{I})\Lambda_r\right]\varepsilon^{\infty}. \tag{18}$$

The effective elastic moduli can then be obtained from the average field in the multi-inclusion

$$\mathbf{C}^* = \mathbf{C}\left[\mathbf{I} + (\mathbf{S} - \mathbf{I})\Lambda\right][\mathbf{I} + \mathbf{S}\Lambda]^{-1} \tag{19}$$

where

$$\Lambda = \sum_{r=1}^{n} f_r \Lambda_r \tag{20}$$

It is clear from Eq. (19) that the effective moduli predicted by the multi-inclusion model depends on the choice of elastic moduli of infinite medium.

3.2. The effective thermal moduli

The effective thermal moduli are related to residual field II, which is solely caused by the temperature

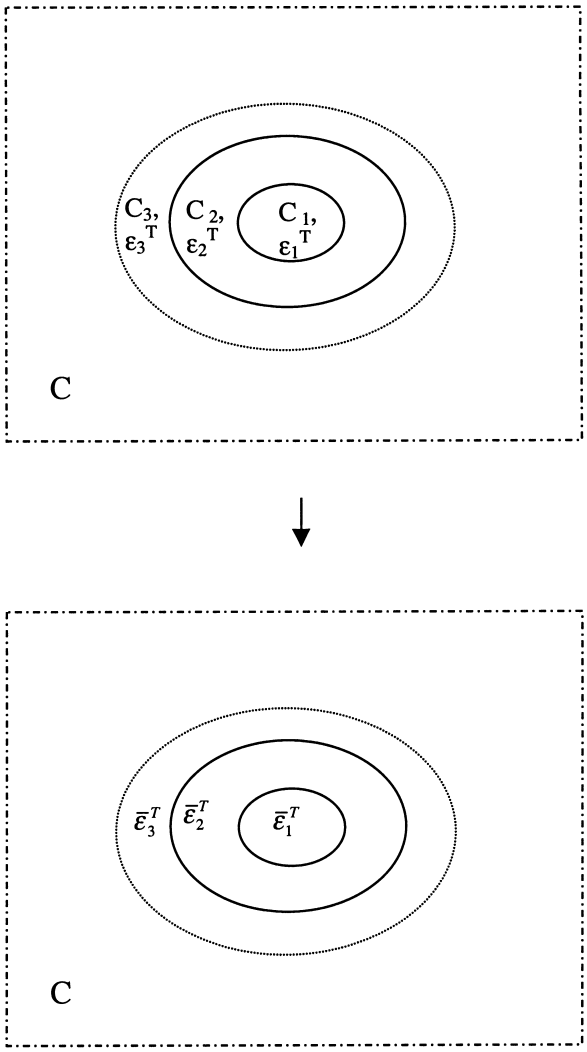

Fig. 2. A multi-inhomogeneity embedded in an infinite medium of elastic moduli **C**, approximated by a multi-inclusion embedded in an infinite medium. The multi-inhomogeneity has elastic moduli $\mathbf{C}_r$ and eigenstrain $\varepsilon_r^{\mathrm{T}}$, and the multi-inclusion has the effective eigenstrain $\bar{\varepsilon}_r^{\mathrm{T}}$.

change θ. Now different phases has not only different elastic moduli, but also different eigenstrain due to the mismatch between thermal moduli, see Fig. 2. The consistent equation for the multi-inclusion and multi-inhomogeneity is then

$$\mathbf{C}_r\left(\varepsilon^{\infty}+\varepsilon_r^{\mathrm{d}}-\varepsilon_r^{\mathrm{T}}\right)=\mathbf{C}\left(\varepsilon^{\infty}+\varepsilon_r^{\mathrm{d}}-\varepsilon_r^{\mathrm{T}}-\varepsilon_r^{**}\right)=\mathbf{C}\left(\varepsilon^{\infty}+\varepsilon_r^{\mathrm{d}}-\varepsilon_r^{*}\right), \tag{21}$$

where $\varepsilon_r^{\mathrm{T}}=-\mathbf{C}_r\boldsymbol{\lambda}_r\theta$ is the eigenstrain in phase r caused by temperature change, and $\varepsilon_r^{*}=\varepsilon_r^{\mathrm{T}}+\varepsilon_r^{**}$ is the equivalent eigenstrain introduced to ensure the correspondence between the multi-inclusion and multi-inhomogeneity. Solving the consistent equation (21), we have

$$\varepsilon_r^{**}=\boldsymbol{\Lambda}_r\varepsilon^{\infty}+\boldsymbol{\Lambda}_r(\mathbf{S}-\mathbf{I})\varepsilon_r^{\mathrm{T}}. \tag{22}$$

The average strain in phase r is then

$$\langle\varepsilon_r^{\mathrm{II}}\rangle=\varepsilon^{\infty}+\mathbf{S}\varepsilon_r^{*}=(\mathbf{I}+\mathbf{S}\Lambda_r)\varepsilon^{\infty}+\mathbf{S}\left[\Lambda_r(\mathbf{S}-\mathbf{I})+\mathbf{I}\right]\varepsilon_r^{\mathrm{T}}. \tag{23}$$

The far-field strain ε^{∞} can be determined from the elastic boundary condition, which has two possibilities. If the boundary is constrained, i.e., no displacement and strain is allowed, then according to the average strain theorem, the average strain in the composite caused by the temperature change should be zero, so that

$$\varepsilon^{\infty}=-(\mathbf{I}+\mathbf{S}\Lambda)^{-1}\sum_{r=1}^{n}f_r\mathbf{S}\left[\Lambda_r(\mathbf{S}-\mathbf{I})+\mathbf{I}\right]\varepsilon_r^{\mathrm{T}}. \tag{24}$$

On the other hand, if the boundary is free, i.e., no traction is applied, from the average stress theorem, the average stress in the composite caused by the temperature change should be zero, so that

$$\varepsilon^{\infty}=-\left[\mathbf{I}+(\mathbf{S}-\mathbf{I})\Lambda\right]^{-1}\sum_{r=1}^{n}f_r(\mathbf{S}-\mathbf{I})\left[\Lambda_r(\mathbf{S}-\mathbf{I})+\mathbf{I}\right]\varepsilon_r^{\mathrm{T}}. \tag{25}$$

The free boundary condition will be used when we study the residual stress in the composite with functionally graded interphase in next section. For the effective thermal stress tensor we only need to consider the constrained boundary condition, and the effective eigenstrain in phase r is

$$\varepsilon_r^{*}=-\Lambda_r(\mathbf{I}+\mathbf{S}\Lambda)^{-1}\mathbf{S}\sum_{r=1}^{n}f_r\left[\Lambda_r(\mathbf{S}-\mathbf{I})+\mathbf{I}\right]\varepsilon_r^{\mathrm{T}}+\left[\Lambda_r(\mathbf{S}-\mathbf{I})+\mathbf{I}\right]\varepsilon_r^{\mathrm{T}}, \tag{26}$$

where Eq. (24) has been used. The effective eigenstrain and the corresponding thermal stress tensor of the composite are then

$$\varepsilon^{*}=(\mathbf{I}+\Lambda\mathbf{S})^{-1}\sum_{r=1}^{n}f_r\left[\Lambda_r(\mathbf{S}-\mathbf{I})+\mathbf{I}\right]\varepsilon_r^{\mathrm{T}} \tag{27}$$

and

$$\lambda^{*}=\mathbf{C}(\mathbf{I}+\Lambda\mathbf{S})^{-1}\sum_{r=1}^{n}f_r\left[\Lambda_r(\mathbf{S}-\mathbf{I})+\mathbf{I}\right]\mathbf{C}_r^{-1}\lambda_r. \tag{28}$$

Again, the effective thermal stress tensor depends on the choice of the elastic moduli of infinite medium.

3.3. Some theoretical consideration

Here we present some theoretical aspects of multi-inclusion model. The first question is whether Eq. (19) is consistent with Eq. (7). To verify this, the connection between the applied strain ε^{∞} at the boundary of infinite medium and the actually applied strain ε^{0} at the boundary of the composite should be established. From the average strain theorem and the average stain in phase r, Eq. (17), we obtained

$$\sum_{r=0}^{n} f_r(\mathbf{I}+\mathbf{S}\Lambda_r)\varepsilon^{\infty}=\varepsilon^{0}, \tag{29}$$

so that

$$\varepsilon^{\infty}=(\mathbf{I}+\mathbf{S}\Lambda)^{-1}\varepsilon^{0}, \tag{30}$$

and finally we obtain the concentration factor

$$\mathbf{A}_r=(\mathbf{I}+\mathbf{S}\Lambda_r)(\mathbf{I}+\mathbf{S}\Lambda)^{-1}. \tag{31}$$

Eq. (31) can be used with Eq. (7) to provide an estimate on the effective elastic moduli, which can be shown to be equivalent to Eq. (19). It can also be used to estimate the average field in phase r, given the boundary condition ε^{0}.

The second question is whether the effective thermal stress tensor predicted by Eq. (28) is consistent with that of Eq. (11), with the concentration factor given by Eq. (31). To answer this question, we first introduce Hill condition (Hill, 1963; Kreher, 1988; Nemat-Nasser and Hori, 1993)

$$\langle\sigma(\mathbf{x})\varepsilon(\mathbf{x})\rangle=\langle\sigma(\mathbf{x})\rangle\langle\varepsilon(\mathbf{x})\rangle, \tag{32}$$

which is valid for linear displacement or uniform traction boundary conditions. The following conditions are used in the derivation: (1) the solid is statistically homogeneous; (2) no body forces exist so that the equilibrium condition is satisfied; (3) strain is derivable from elastic displacement. The strain tensor ε and stress tensor σ need not be connected by certain constitutive equation. Hill condition, combined with average strain theorem, gives us

$$\langle\sigma^{\mathrm{II}}(\mathbf{x})\varepsilon^{\mathrm{I}}(\mathbf{x})\rangle=\langle\sigma^{\mathrm{II}}(\mathbf{x})\rangle\langle\varepsilon^{\mathrm{I}}(\mathbf{x})\rangle=\lambda^{*}\theta\varepsilon^{0}. \tag{33}$$

On the other hand, from the phase constitutive equation we obtain

$$\langle\sigma^{\mathrm{II}}(\mathbf{x})\varepsilon^{\mathrm{I}}(\mathbf{x})\rangle=\langle\sigma^{\mathrm{I}}(\mathbf{x})\varepsilon^{\mathrm{II}}(\mathbf{x})\rangle+\langle\lambda(\mathbf{x})\theta\varepsilon^{\mathrm{I}}(\mathbf{x})\rangle, \tag{34}$$

The two equations combined yields

$$\lambda^{*}\theta\varepsilon^{0}=\langle\lambda(\mathbf{x})\theta\varepsilon^{\mathrm{I}}(\mathbf{x})\rangle. \tag{35}$$

Using the definition of the concentration factor, we finally obtained

$$\lambda^{*}=\langle\mathbf{A}^{\mathrm{T}}(\mathbf{x})\lambda(\mathbf{x})\rangle, \tag{36}$$

which is consistent with Eq. (11).

A desirable property of the multi-inclusion model is its connections with other micromechanics approaches. As shown by Nemat-Nasser and Hori (1993), the effective elastic moduli predicted by multi-inclusion model can correspond to the Mori and Tanaka (1973) approach, the self-consistent approach (Hill, 1965), and Hashin and Shtrikman (1962, 1963) upper and lower bounds, if the elastic moduli of

the matrix, of the yet unknown effective moduli, or the elastic moduli stiffer or softer than the constituent materials of the composite, is assigned to the infinite medium. The multi-inclusion model thus provide a uniform framework for the micromechanical analysis of heterogeneous materials.

4. Composites with functionally graded interphase

Now let us apply the multi-inclusion model to composite materials with functionally graded interphase. By functionally graded interphase we refer to an interphase with continuously varying properties between matrix and reinforcement, as shown in Fig. 3. Phase 1 is the reinforcement, phase 3 is the matrix, both having homogeneous material properties. Phase 2, the interphase, however, has spatially varying material properties. The reinforcement is considered to be perfectly aligned and ellipsoidally shaped with dimensions a_1, b_1, c_1, and a_2, b_2, c_2. The ellipsoids are coaxial and of similar shape so that $\frac{a_1}{a_2} = \frac{b_1}{b_2} = \frac{c_1}{c_2} = \gamma$. For a given composite, only γ need to be fixed while the actual dimension of the interphase can be varied. The volume fraction of matrix is f_3, and the volume fraction of phase 1 and 2 can be obtained as $f_1 = (1-f_3)\frac{a_1b_1c_1}{a_2b_2c_2} = (1-f_3)\gamma^3$ and $f_2 = (1-f_3)(1-\gamma^3)$. Statistical homogeneity is assumed for the composite material. The spatially varying material properties of the interphase present a challenge to traditional micromechanics approximations. This problem, however, can be solved by multi-inclusion model. The fields in phase 1 and 3 can be analyzed in an identical manner as in the last section; the field in the interphase 2 requires more analysis. As in the last section, we will first consider the loading field due to the applied linear displacement boundary condition, and then analyze the residual field due to the temperature change.

4.1. Loading field under the applied displacement

We assume the elastic moduli $\mathbf{C}_2(r)$ is a radial function, so are the equivalent eigenstrain $\bar{\varepsilon}_2^{\mathrm{T}}(r)$ and the disturbance field $\varepsilon_2^{\mathrm{d}}(r)$, where r represents the normalized radial distance from the inner surface of the interphase ranging from γ to 1. For an infinite small range dr, the material properties are considered to be uniform so that Eq. (12) is still valid. The consistent equation (14) between the multi-inclusion and multi-inhomogeneity thus gives us

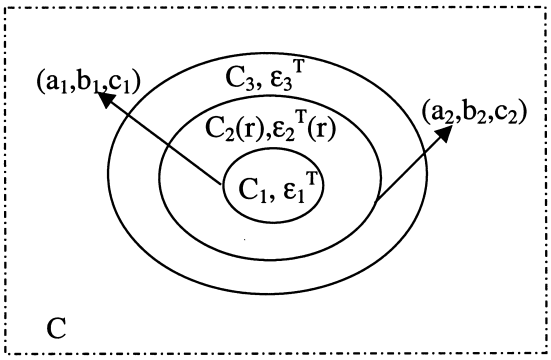

Fig. 3. A composite with functionally graded interphase between reinforcement 1 and matrix 3. The dimension of reinforcement and interphase are a_1, b_1, c_1, and a_2, b_2, c_2.

$$\bar{\varepsilon}_2^{\mathrm{T}}(r) = \Lambda_2(r)\varepsilon^{\infty}, \tag{37}$$

where

$$\Lambda_2(r) = \left\{\left[\mathbf{C} - \mathbf{C}_2(r)\right]^{-1}\mathbf{C} - \mathbf{S}\right\}^{-1}. \tag{38}$$

The spatial distribution of strain and stress in the interphase are then

$$\varepsilon_2^{\mathrm{I}}(r) = \left[\mathbf{I} + \mathbf{S}\Lambda_2(r)\right]\varepsilon^{\infty} \tag{39}$$

and

$$\sigma_2^{\mathrm{I}}(r) = \mathbf{C}\left[\mathbf{I} + (\mathbf{S} - \mathbf{I})\Lambda_2(r)\right]\varepsilon^{\infty}. \tag{40}$$

The average disturbance strain $\langle\varepsilon_2^{\mathrm{d}}(r)\rangle$ in phase 2 is then

$$\begin{aligned}\langle\varepsilon_2^{\mathrm{d}}(r)\rangle &= \frac{1}{\frac{4}{3}\pi(a_2b_2c_2 - a_1b_1c_1)}\int_{c1}^{c2}\int_{b1}^{b2}\int_{a1}^{a2}\mathbf{S}\bar{\varepsilon}_2^{\mathrm{T}}(r)\,\mathrm{d}x\,\mathrm{d}y\,\mathrm{d}z = \frac{3\mathbf{S}}{1-\gamma^3}\int_{\gamma}^{1} r^2\bar{\varepsilon}_2^{\mathrm{T}}(r)\,\mathrm{d}r \\ &= \frac{3\mathbf{S}}{1-\gamma^3}\int_{\gamma}^{1} r^2\Lambda_2(r)\,\mathrm{d}r\varepsilon^{\infty}.\end{aligned} \tag{41}$$

Let

$$\bar{\Lambda}_2 = \frac{3}{1-\gamma^3}\int_{\gamma}^{1} r^2\Lambda_2(r)\,\mathrm{d}r, \tag{42}$$

Eqs. (19) and (31) can then be applied to the composite materials with functionally graded interphase, with Λ_2 replaced by $\bar{\Lambda}_2$ given by Eq. (42), to estimate the effective elastic moduli and analyze the internal field distribution in the composite due to the applied linear displacement at the boundary. Two limiting cases immediately follow, one is when γ approaches zero and phase 1 disappears; the other is when γ approaches unit and there is no interphase between the matrix and reinforcement.

4.2. Residual field due to the temperature change

The analysis of residual field in the interphase due to the temperature change is a little bit more complicated, but can be pursued in a similar manner. Again, we assume $\mathbf{C}_2(r)$ and $\lambda_2(r)$ to be radial functions. The spatial distribution of residual strain and stress in the interphase are then

$$\varepsilon_2^{\mathrm{II}}(r) = \varepsilon^{\infty} + \mathbf{S}\varepsilon_2^{*}(r) = \left[\mathbf{I} + \mathbf{S}\Lambda_2(r)\right]\varepsilon^{\infty} + \mathbf{S}\left[\Lambda_2(r)(\mathbf{S} - \mathbf{I}) + \mathbf{I}\right]\varepsilon_2^{\mathrm{T}}(r). \tag{43}$$

and

$$\sigma_2^{\mathrm{II}}(r) = \mathbf{C}\left[\mathbf{I} + (\mathbf{S} - \mathbf{I})\Lambda_2(r)\right]\left[\varepsilon^{\infty} + (\mathbf{S} - \mathbf{I})\varepsilon_2^{\mathrm{T}}(r)\right]. \tag{44}$$

If we define

$$\overline{\left[\Lambda_2(\mathbf{S} - \mathbf{I}) + \mathbf{I}\right]\varepsilon_2^{\mathrm{T}}} = \frac{3}{1-\gamma^3}\int_{\gamma}^{1} r^2\left[\Lambda_2(r)(\mathbf{S} - \mathbf{I}) + \mathbf{I}\right]\varepsilon_2^{\mathrm{T}}(r)\,\mathrm{d}r, \tag{45}$$

Table 1
Numerical procedure of multi-inclusion model for composites with functionally graded interphase

Step	Operation
1	Input the constituent properties of the reinforcement ($\mathbf{C}_1$ and λ_1), the matrix ($\mathbf{C}_3$ and λ_3), and the properties of the infinite medium ($\mathbf{C}$).
2	Input the volume fraction f_3, the normalized thickness of the interphase γ, and inclusion aspect ratio β. Evaluate the volume fraction f_1 and f_2 using the interphase thickness γ.
3	Evaluate the properties of the interphase [$\mathbf{C}_2(r)$ and $\lambda_2(r)$] according to specified property profile.
4	Evaluate the Eshelby tensor $\mathbf{S}$ using the elastic property ($\mathbf{C}$) of the infinite medium and the inclusion shape aspect ratio β.
5	Evaluate Λ_1, Λ_3, $\Lambda_2(r)$ according to Eq. (16), using MATHEMATICA build-in function *Inverse*.
6	Evaluate $\bar{\Lambda}_2$ according to Eq. (42), using MATHEMATICA build-in function *NIntegrate*.
7	Evaluate the effective elastic moduli $\mathbf{C}^*$ according to Eqs. (19) and (20).
8	Evaluate concentration factor $\mathbf{A}_2(r)$ according to Eq. (31), and corresponding internal stress $\sigma_2^{\mathrm{I}}(r)$ according to Eq. (8).
9	Evaluate $\overline{[\Lambda_2(\mathbf{S}-\mathbf{I})+\mathbf{I}]\varepsilon_2^{\mathrm{T}}}$ according to Eq. (45), using MATHEMATICA build-in function *NIntegrate*.
10	Evaluate the effective thermal stress tensor λ^* according to Eq. (28).
11	Evaluate residual stress $\sigma_2^{\mathrm{II}}(r)$ according to Eq. (44), where ε^{∞} is evaluated by Eq. (24) or (25), depending on the boundary condition.

Table 2
Comparison on the thickly-coated particle and fiber-reinforced composites; the Young's modulus of the matrix, inclusion, and the coating are 1, 25, and 5 GPa, respectively, and the Possion ratio is 0.3 for all phases. The elastic moduli of the reinforcement and matrix are assigned to the infinite medium in model 1 and 2, respectively

	Bulk modulus (GPa)		Axial shear modulus(GPa)	
	$c_1/c_2/c_3 = 0.7/0.2/0.1$	$c_1/c_2/c_3 = 0.1/0.2/0.7$	$c_1/c_2/c_3 = 0.7/0.2/0.1$	$c_1/c_2/c_3 = 0.7/0.2/0.1$
	Particulate composite		Fibrous composite	
Hashin–Shtrikman upper bound	12.24	2.33	6.07	1.19
Hashin–Shtrikman lower bound	6.16	1.25	3.10	0.61
Qiu and Weng (1991)	6.47	1.26	3.33	0.62
Multi-inclusion model 1	12.24	2.328	6.075	1.192
Multi-inclusion model 2	6.162	1.250	3.104	0.609

then Eqs. (24), (27) and (28) are still valid, with Λ_2 replaced by $\bar{\Lambda}_2$ given by Eq. (42), and $[\Lambda_2(\mathbf{S}-\mathbf{I})+\mathbf{I}]\varepsilon_2^{\mathrm{T}}$ replaced by $[\bar{\Lambda}_2(\mathbf{S}-\mathbf{I})+\mathbf{I}]\varepsilon_2^{\mathrm{T}}$ given by Eq. (45). The thermal field and effective thermal stress tensor can then be obtained. Depending on whether the boundary is free or constrained, Eqs. (25) and (24) will be used for ε^{∞}. We also note that the temperature need not to be uniform in the composite, and its spatial variation can be reflected in $\varepsilon_2^{\mathrm{T}}(r)$, if the temperature distribution is determined from the heat conduction problem (when it is uncoupled from the deformation). So the effect of temperature gradient can be analyzed in this framework without difficulty.

5. Numerical results and discussion

To demonstrate our theory we will show some numerical results in this section. The numerical computation is implemented in a MATHEMATICA program, which is outlined in Table 1. In order to verify the program, we have compared our calculations with some previous results by Qiu and Weng (1991), who obtained the effective moduli of thickly coated particle and fiber-reinforced composites by the replacement method and the Hashin–Shtrikman upper and lower bounds. The materials they considered correspond to a special class of functionally graded interphase which has uniform material properties. The comparison between results from their calculations and the multi-inclusion model is listed in Table 2. It is found that when we assign the moduli of matrix and reinforcement to the infinite medium, the multi-inclusion model agrees with the Hashin–Shtrikman lower and upper bounds, respectively. Qiu and Weng's results are close to the lower bound, because the matrix is the softest phase in the composite.

Table 3
Material properties of SiC reinforcement and intermetallic matrix

	C_{11} (GPa)	C_{12} (GPa)	α_{11} ($10^{-6}/^{\circ}$C)
SiC	504	150	4.86
Intermetallic matrix	176.67	103.67	9.25

We then consider the SiC reinforced intermetallic matrix (Ti-24A1-11Nb). There is a interphase between the reinforcement and matrix, with material properties (elastic moduli and thermal expansion coefficient) change linearly from the reinforcement properties to matrix properties (see Fig. 3), which are listed in Table 3 (Huang and Rokhlin, 1996). Other property profile of the interphase can be studied but will not be presented here. The volume fraction of matrix is fixed at 60%, although its effect can also be investigated. We will first fix the inclusion thickness, and consider the effect of inclusion aspect ratio $\beta = \frac{c_1}{a_1} = \frac{c_1}{b_1}$ on the effective moduli. The effect of normalized interphase thickness $1-\gamma$ will then be studied with fixed inclusion aspect ratio. Two composite geometries will be considered, one is perfectly aligned circular cylindrical fiber reinforced, and the other is spherical particle reinforced. Both effective thermoelastic moduli and thermoelastic field will be studied. In the calculation, the elastic moduli of matrix and reinforcement are assigned to the infinite medium, so that the effective elastic moduli obtained correspond to the lower and upper bounds on the effective moduli of the composite.

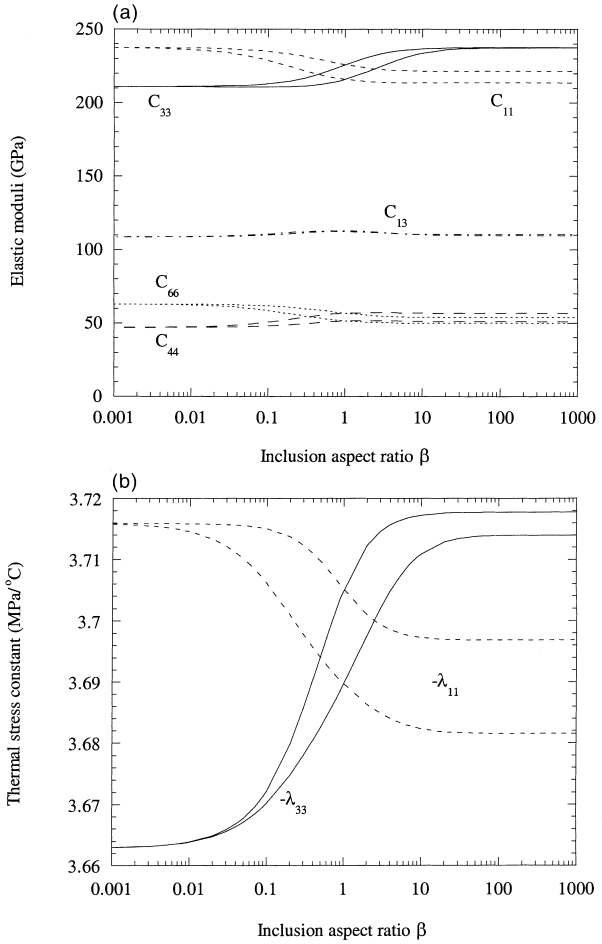

Fig. 4. The effective thermoelastic moduli of composite with functionally graded interphase as function of inclusion aspect ratio β: (a) elastic moduli; (b) thermal moduli.

5.1. The effective thermoelastic moduli

We first present the effective thermoelastic moduli of the composite as function of inclusion aspect ratio β in Fig. 4, where (a) is for effective elastic moduli, and (b) is for effective thermal moduli. The normalized interphase thickness is 0.5. It is found that C_{11}, C_{66}, and $-\lambda_{11}$ decrease with the inclusion aspect ratio β, while C_{33}, C_{44}, and $-\lambda_{33}$ increase with it. Zero and infinity aspect ratio of the inclusion correspond to the laminated and fibrous composites, in which C_{33} is exact, verified by the agreement of the upper and lower bounds. Other effective moduli are exact for laminated composite, but not for the fibrous composite, as is clear from the figures. None of the moduli is exact for composites other than these two special cases. We then present the effective thermoelastic moduli of the composite as function of normalized interphase thickness. Figs. 5 and 6 show the effective elastic stiffness tensor and effective thermal stress tensor; (a) is for fibrous composite, while (b) is for particulate composite. Since all the constituents are isotropic, so are the particulate composite; the fibrous composite is transversely

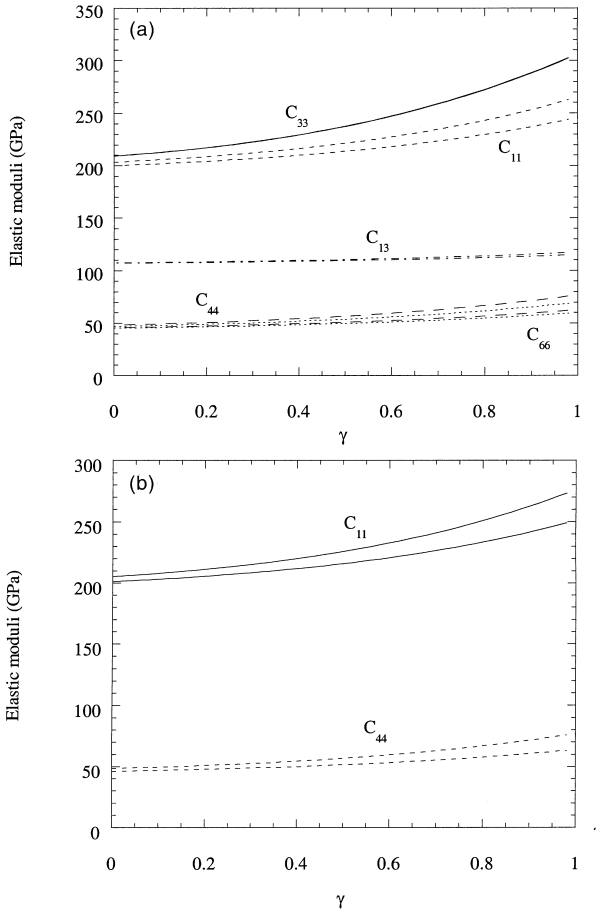

Fig. 5. The effective elastic moduli of composite with functionally graded interphase as function of normalized interphase thickness $1-\gamma$: (a) fibrous composite; (b) particulate composite.

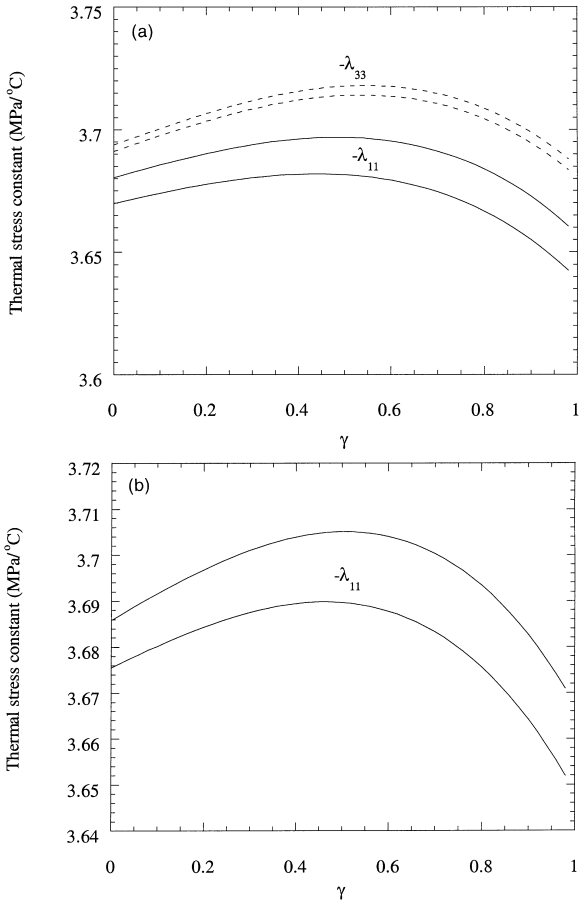

Fig. 6. The effective thermal expansion coefficients of composite with functionally graded interphase as function of normalized interphase thickness $1-\gamma$: (a) fibrous composite; (b) particulate composite.

isotropic, however. From the figures, it is found that the upper and lower bounds on all the components are very close to each other, especially for C_{33} and C_{13} of fibrous composite. It is noted that C_{13} is actually not bounded because it is a off-diagonal component. Except for C_{13}, which is not much affected by the interphase thickness γ, all other elastic moduli vary significantly with respect to the change in γ. All the elastic moduli increase with γ, because with volume fraction of matrix fixed, increased γ represents increased volume fraction of reinforcement, which is stiffest constituent in the composite. The effective thermal stress tensor, however, show a peak with respect to the change in γ. It increases initially, and then drops. Its variation with respect to γ is much less prominent than that of elastic moduli.

5.2. Loading and residual thermoelastic field

Here we fix the γ to be 0.5, and study the field variation in interphase with respect to different loading condition. We first considered the applied tensile loading in x_1 and x_3 direction. For particulate

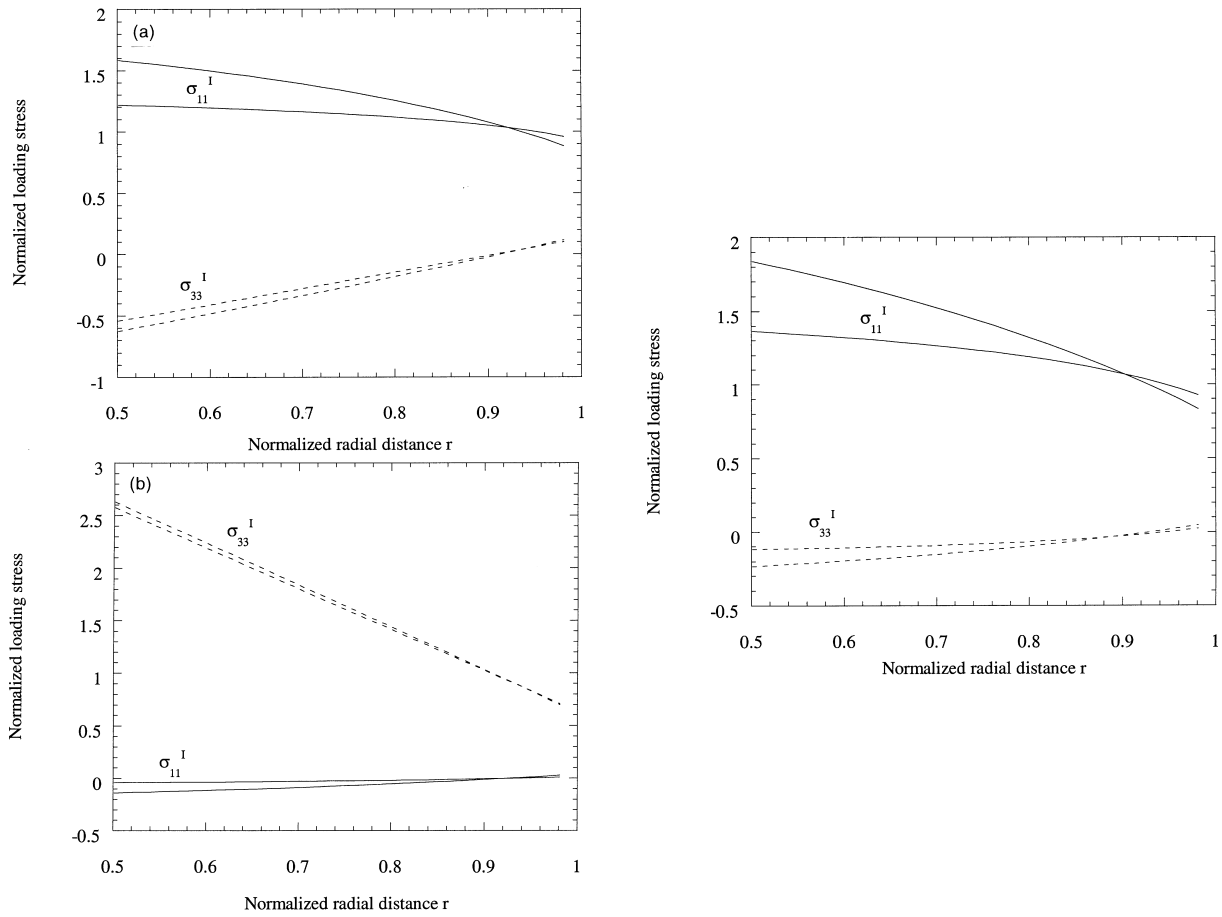

Fig. 7. Loading stress in the interphase as function of radial distance from reinforcement: (a) applied σ_{11} in the fibrous composite; (b) applied σ_{33} in the fibrous composite; (c) applied σ_{11} in the particulate composite.

composite, these two loading conditions produce equivalent result due to symmetry, as shown in Fig. 7(c). When it is applied along x_1 axis, σ_{11} decrease with the increase of r, because the stiffness of the interphase decreases. σ_{33}, however, changes from compression state to tensile state. This is because the interaction between constituents and the Poisson ratio effect. Although the difference between the effective moduli is small when different elastic moduli is assigned to infinite medium, the difference between the resulting loading fields is quite large. For the fibrous composite, when the applied loading is along x_1 axis, as shown in Fig. 7(a), the observation is similar to the particulate composite, although larger stress is produced in x_3 direction. When the loading is along x_3 direction, as shown in Fig. 7(b), σ_{33} decrease with increase of r linearly, while σ_{11} changes from compressive state to tensile state.

Now let us consider the thermal stress variation in the interphase. The boundary of the composite is assumed to be free so that no traction is applied. Fig. 8(a and b) show the thermal stress variation in fibrous and particulate composites, respectively. Because the reinforcement has less thermal expansion coefficient than the matrix, and due to the constraint between different phases, there are tensile stress in

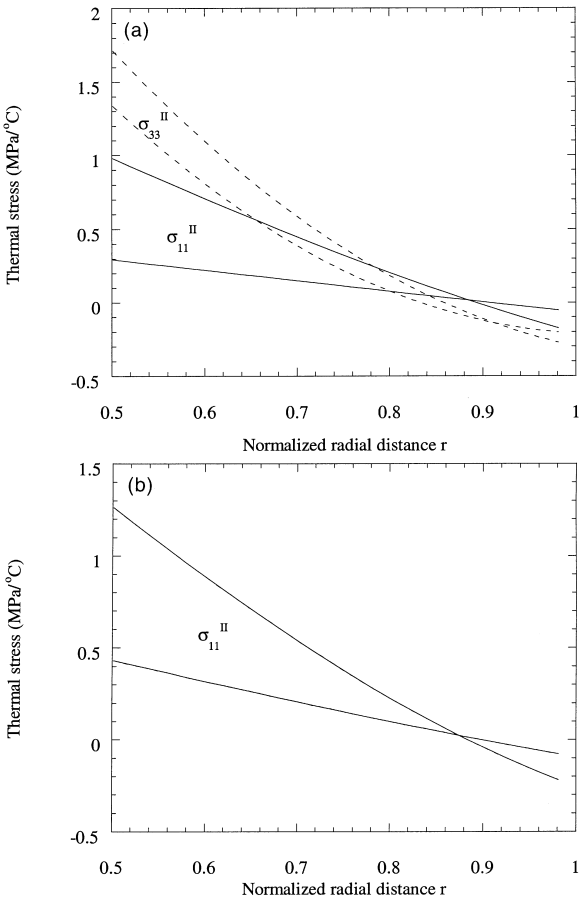

Fig. 8. Residual field in the interphase as function of radial distance from reinforcement: (a) fibrous composite; (b) particulate composite.

the reinforcement, and compression stress in the matrix. In the interphase, the residual stresses drop with increase of the radial distance from the reinforcement. Due to the symmetry, the σ_{11} and σ_{33} are same in the particulate composite. In the fibrous composite, however, σ_{33} is much larger than σ_{11}.

6. Concluding remarks

A multi-inclusion model is developed to study the thermoelastic behavior of composite materials with functionally graded interphase. The properties of the interphase can be varied in an arbitrary manner between reinforcement and matrix, and there could be a thermal gradient in the interphase. Explicit expressions for the effective thermoelastic moduli and thermoelastic field are obtained, and numerical results for SiC reinforced intermetallic matrix are presented and discussed.

Acknowledgements

The support and encouragement of Dr. Nemat-Nasser is gratefully acknowledged.

References

Aboudi, J., Pindera, M.J., 1996. Thermoelastic theory for the response of materials functionally graded in two directions. Int. J. Solids Structures 33, 931–966.

Benveniste, Y., Dvorak, G.J., Chen, T., 1989. Stress fields in composites with coated inclusions. Mechanics of Materials 7, 305–317.

Benveniste, Y., Dvorak, G.J., Chen, T., 1991. On diagonal and elastic symmetry of the approximate effective stiffness tensor of heterogeneous media. J. Mech. Phys. Solids 39, 927–946.

Christensen, R.M., Lo, K.H., 1979. Solutions for effective shear properties of three-phase sphere and cylinder models. J. Mech. Phys. Solids 27, 315–330.

Chu, Y.C., Rokhlin, S.I., 1995. Determination of fiber–matrix interphase moduli from experimental moduli of composite with multi-layered fibers. Mechanics of Materials 21, 191–215.

Dao, M., Gu, P., Maewal, A., Asaro, R.J., 1997. A micromechanical study of residual stresses in functionally graded materials. Acta Mater 45, 3265–3276.

Delfosse, D., Cherradi, N., Ilschner, B., 1997. Numerical and experimental determination of residual stresses in graded materials. Composites B 28B, 127–141.

Dunn, M.L., Ledbetter, H., 1995. Elastic moduli of composites reinforced by multiphase particles. Journal of Applied Mechanics 62, 1023–1028.

Eshelby, J.D., 1957. The determination of the elastic field of an ellipsoidal inclusion, and related problems. Proc. R. Soc. Lond. A 241, 376–396.

Hashin, Z., 1990. Thermoelastic properties of fiber composites with imperfect interphase. Mechanics of Materials 8, 333–348.

Hashin, Z., Rosen, B.W., 1964. The elastic moduli of fiber-reinforced materials. J. Appl. Mech 31, 223–232.

Hashin, Z., Shtrikman, T., 1962. A variational approach to the elastic behavior of polycrystals. J. Mech. Phys. Solids 10, 343–352.

Hashin, Z., Shtrikman, T., 1963. A variational approach to the theory of the elastic behavior of multiphase materials. J. Mech. Phys. Solids 11, 127–140.

Hill, R., 1963. Elastic properties of reinforced solids: some theoretical principles. J. Mech. Phys. Solids 11, 357–372.

Hill, R., 1965. A self-consistent mechanics of composite materials. J. Mech. Phys. Solids 13, 213–222.

Hori, M., Nemat-Nasser, S., 1994. Double-inclusion model and overall moduli of multi-phase composites. Journal of Engineering Materials and Technology 116, 305–309.

Huang, W., Rokhlin, S.I., 1996. Generalized self-consistent model for composites with functionally graded and multilayered interphase, transfer matrix approach. Mechanics of Materials 22, 219–247.

Kreher, W., 1988. Internal stresses and relations between effective thermoelastic properties of stochastic solids—some exact solutions. Z. Angew. Math. Mech 68, 147–154.

Levin, V.M., 1967. On the coefficients of thermal expansion of heterogeneous materials. Mekh. Tverdogo Tela, 88–94.

Li, J.Y., 1999. On micromechanics approximation for the effective thermoelastic moduli of multi-phase composite materials. Mechanics of Materials 31, 149–159.

Li, J.Y., Dunn, M.L., 1999. Analysis of microstructural fields in heterogeneous piezoelectric solids. International Journal of Engineering Science 37, 665–685.

Lutz, M.P., Ferrari, M., 1995. Effect of an inhomogeneous interphase region on the mechanical properties of a fiber composite. In: Proceedings of Topical Symposium III on Advanced Structural Fiber Composites of the 8th CIMTEC-World Ceramics Congress and Forum on New Materials, Faenza, Italy, TECHNA, 559–566.

Markworth, A.J., Ramesh, K.S., Parks, W.P., 1995. Modeling studies applied to functionally graded materials. Journal of Materials Science 30, 2183–2193.

Mori, T., Tanaka, K., 1973. Average stress in matrix and average elastic energy of materials with misfitting inclusions. Acta Metall 21, 571–574.

Nemat-Nasser, S., Hori, M., 1993. Micromechanics: Overall Properties of Heterogeneous Materials. Elsevier, North-Holland, Amsterdam.

Noda, N., Nakai, S., 1998. Thermal stresses in functionally graded material of particle-reinforced composite. JSME International Journal A 41, 178–184.

Qiu, Y.P., Weng, G.J., 1991. Elastic moduli of thickly coated particle and fiber-reinforced composites. J. Appl. Mech 58, 388–398.

Rosen, B.W., Hashin, Z., 1970. Effective thermal expansion coefficients and specific heats of composite materials. Int. J. Eng. Sci 8, 157–173.

Shaw, L.L., 1998. Thermal residual stresses in plates and coatings composed of multi-layered and functionally graded materials. Composites B 29B, 199–210.

Tanaka, K., Mori, T., 1972. Note on volume integrals of the elastic field around an ellipsoidal inclusion. Journal of Elasticity 2, 199–200.